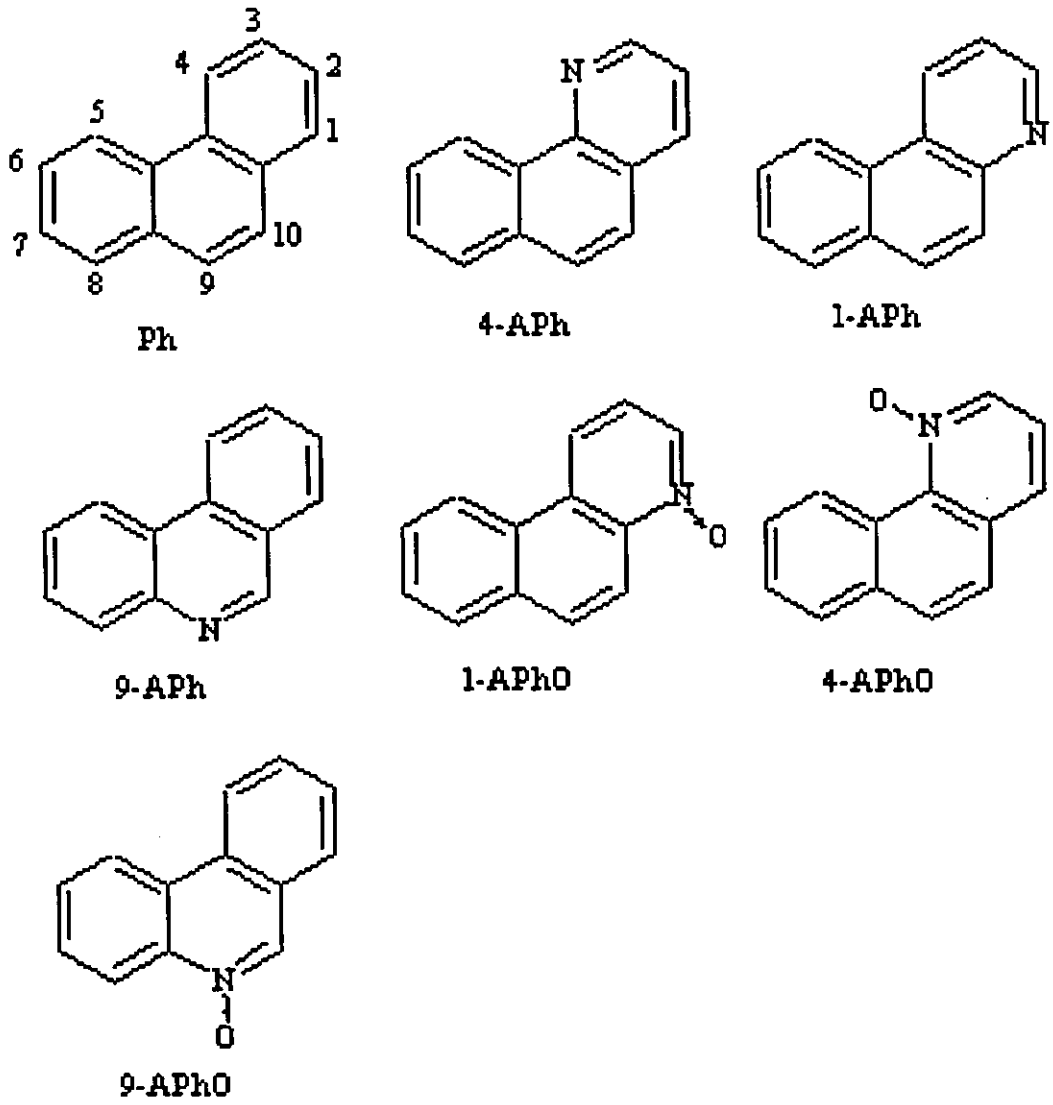

FIGURE 1. Chemical structures of phenanthrenes and their related compounds: APh, azaphenanthrene; APhO, azaphenanthrene N-oxide.

19 NAPhs, including their N-oxide derivatives, were synthesized; 1-, 3-, and 9-NPhs; 1,5-, 1,6-, 1,10-, 2,6-, 2,9-, 2,10-, 3,5-, 3,6-, 3,10-, 4,9-, and 4,10-diNPhs; 1,5,9-, 1,5,10-, 1,6,9-, 1,7,9-, 2,5,10-, 2,6,9-, 3,5,10-, and 3,6,9-triNPhs; 8-N-1-ANPh, 6- and 8-N-4-APhs, 4-, 5-, 6-, and 7-N-9-APhs; 5-, 6-, and 8-N-1-APhOs, 5-, 6-, and 8-N-4-APhOs, 1-, 2-, 3-, and 5-N-9-APhOs; 1,5- and 1,8-diN-4-APhOs. Tables 1 and 2 indicate the results for reduction potentials, LUMO energy levels, and orientation of NPhs and NAPhs. As shown in Table 1, NPhs substituted at the 1 and 8, 5 and 4, 9 and 10 positions in the phenanthrene rings were perpendicular or almost perpendicular due to the steric effect of the bay region aromatic proton, while those at the 2 and 7, 3 and 6 positions were almost

TABLE 1. LUMO Energy Levels and Dihedral Angles of Nitrophenanthrenes

Compound	Epc	LUMO	Dihedral angles (deg)
1-NPh	−1,477	−1.345	16.9
3-NPh	−1,453	−1.367	0.3
9-NPh	−1,450		11.1
1,5-diNPh	−1,373	−1.644	125
1,6-diNPh	−1,357	−1.937	19.1
1,10-diNPh	−1,336	−1.767	127.5
2,6-diNPh	−1,365	−1.836	2.8
2,9-diNPh	−1,311	−1.908	17.9
2,10-diNPh	−1,368	−1.901	15.7
3,5-diNPh	−1,363	−1.735	87.3
3,6-diNPh	−1,341	−1.955	0.5
3,10-diNPh	−1,242	−2.006	18.8
4,9-diNPh	−1,277	−1.880	112.7
4,10-diNPh	−1,297	−1.850	110.2
1,5,9-triNPh	−1,063	−2.345	151.6
1,5,10-triNPh	−1,150	−2.228	198.1
1,6,9-triNPh	−1,058	−2.528	51.6
1,7,9-triNPh	−1,058	−2.422	57.8
2,5,10-triNPh	−1,050	−2.186	174.3
2,6,9-triNPh	−1,116	−2.432	35.7
3,5,10-triNPh	−1,139	−2.394	122.1
3,6,9-triNPh	−1,042	−2.643	21.2

coplanar to the phenanthrene rings, showing dihedral angles from 0.3 to 2.8. Similarly, the chemical properties of NAPhs were also calculated, as shown in Table 2. NAPhs substituted at the 2 and 7, and 3 and 6 were almost coplanar, showing dihedral angles from 0.0 to 0.7 while those at the 1, 4, 5, and 8 were perpendicular or almost perpendicular to the aromatic rings. In addition, the calculated LUMO energy levels were in good correlation with the observed reduction potentials among NPhs and NAPhs; in particular, the LUMO energy levels were correlated with the first reduction potentials more than the second reduction potentials (Table 2).

As this study was to investigate whether or not these chemical properties were associated with 8-oxo-Gua formation in primary rat hepatocytes. Primary rat hepatocytes were prepared from male SD rats as described in the Materials and Methods section. The ability to form 8-oxo-Gua in the primary rat hepatocytes was investigated using 4-NQO, a potent carcinogen. The results were obtained with dose dependency for

TABLE 2. LUMO Energy Levels, Reduction Potentials, and Dihedral Angles of Nitroazaphenanthrenes

	Epc (mV)			
Chemical	Epc1	Epc2	LUMO	Dihedral angle
8-N-1-Aph	−1,042	−1,631	−1,429	31.5
6-N-4-Aph	−1,036	−1,675	−1,400	0.1
8-N-4-Aph	−1,058	1,555	−1,372	32.2
4-N-9-Aph	−1,120	−1,662	−1,326	62.6
5-N-9-Aph	−1,085	−1,615	−1,219	61.7
6-N-9-Aph	−1,027	−1,645	−1,508	0.2
7-N-9-Aph	−1,004	−1,664	−1,436	0
5-N-1-APhO	−1,049	−1,625	−1,505	61
6-N-1-APhO	−972	−1,572	−1,663	0.1
8-N-1-APhO	−988	−1,641	−1,623	33.3
5-N-4-APhO	−1,214	−1,619	−1,427	32.2[a]
6-N-4-APhO	−1,059	−1,723	−1,583	0.7
8-N-4-APhO	−1,047	−1,678	−1,545	31.7
1-N-9-APhO	−853	−1,484	−1,674	26.5
2-N-9-APhO	−964	−1,628	−1,696	0.1
3-N-9-APhO	−893	−1,463	−1,733	0.1
5-N-9-APhO	−1,029	−1,568	−1,494	60.3
1,5-diN-4-APho	−623	−1,263	−2,074	30.1[b]
1,8-diN-4-APho	−916	−1,032	−2,214	58.2*

*8-NO2, 33.5; 1-NO2, 24.7.

[a,b]LUMO energy and dihedral angle were obtained by AM1 calculations based on the structure that was optimized by PM3.

8-oxo-Gua formation at dose levels from 1 to 5 nM of 4-NQO (Figure 2), suggesting metabolic activation of cytochrome p450 in rat hepatocytes.

Figure 3 shows the correlation between the first reduction potentials of NPhs (a) and LUMO energy (b), and levels of 8-oxo-Gua formed in rat hepatocytes. The first reduction potentials of NPhs, but not the second reduction potentials, represented a significant correlation with 8-oxo-Gua levels ($r = 0.906$) (Figure 3a). In addition, the correlation between LUMO energy and 8-oxo-Gua levels was analyzed (Figure 3b). It was found that 8-oxo-Gua was strongly formed at lower LUMO energy levels from −1.345 to −2.643, and both agents were significantly correlated at a correlation factor of 0.874.

The first reduction potentials and LUMO energy levels of NAPhs were also determined, and the results are illustrated in Figure 4. Similarly, the first reduction potentials were involved with the metabolic reduction of the nitro group of PAHs and the involvement was more pronounced than

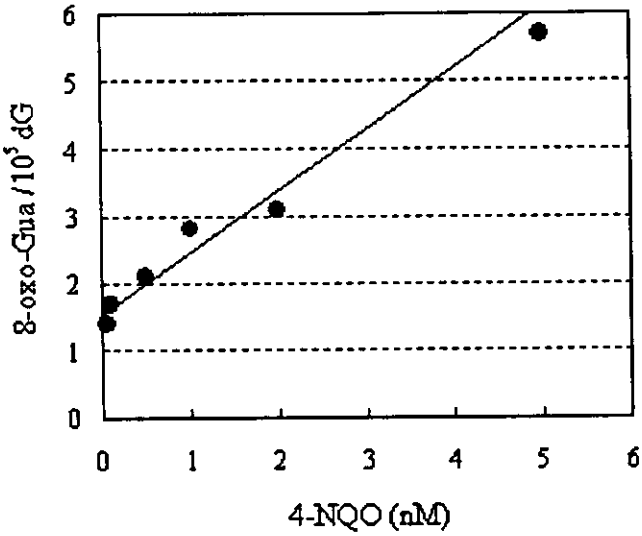

FIGURE 2. 8-oxo-Gua formation by 4-NQO in primary rat hepatocytes.

the second reduction potentials (data not shown). The first reduction potentials of mononitro-APhs were lower than those of dinitro-APhs (Table 2).

The 8-oxo-Gua formation of NPhs was significantly correlated with the first reduction potentials ($r = 0.924$) and also with LUMO energy levels, but was not significant ($r = 0.428$). The 8-oxo-Gua formation increased at the higher levels of the first reduction potentials, but was at lower levels of LUMO energy (Figure 4a, b).

Possible Mechanism of Oxygen Damage Due to NPhs and NAPhs

Modification of guanine residue on DNA due to oxygen damage was analyzed, and its chemical pathway is illustrated in Figure 5. Nitro groups of NPhs and NAPhs were metabolically reduced by the NADPH-cytochrome p450 enzyme in primary rat hepatocytes, and radical anions were induced at the 8-position of the guanine residue. Subsequently, reactive oxygen species as superoxides were generated, and hydroxyl radicals were generated in the presence of heme iron. Consequently, it was considered that 8-oxo-Gua was formed by the reactive hydroxyl radical at position 8 of the guanine residue.

DISCUSSION

We previously reported that the mutagenic potency of NPhs and NAPhs for *Salmonella* strains was closely correlated with the orientation

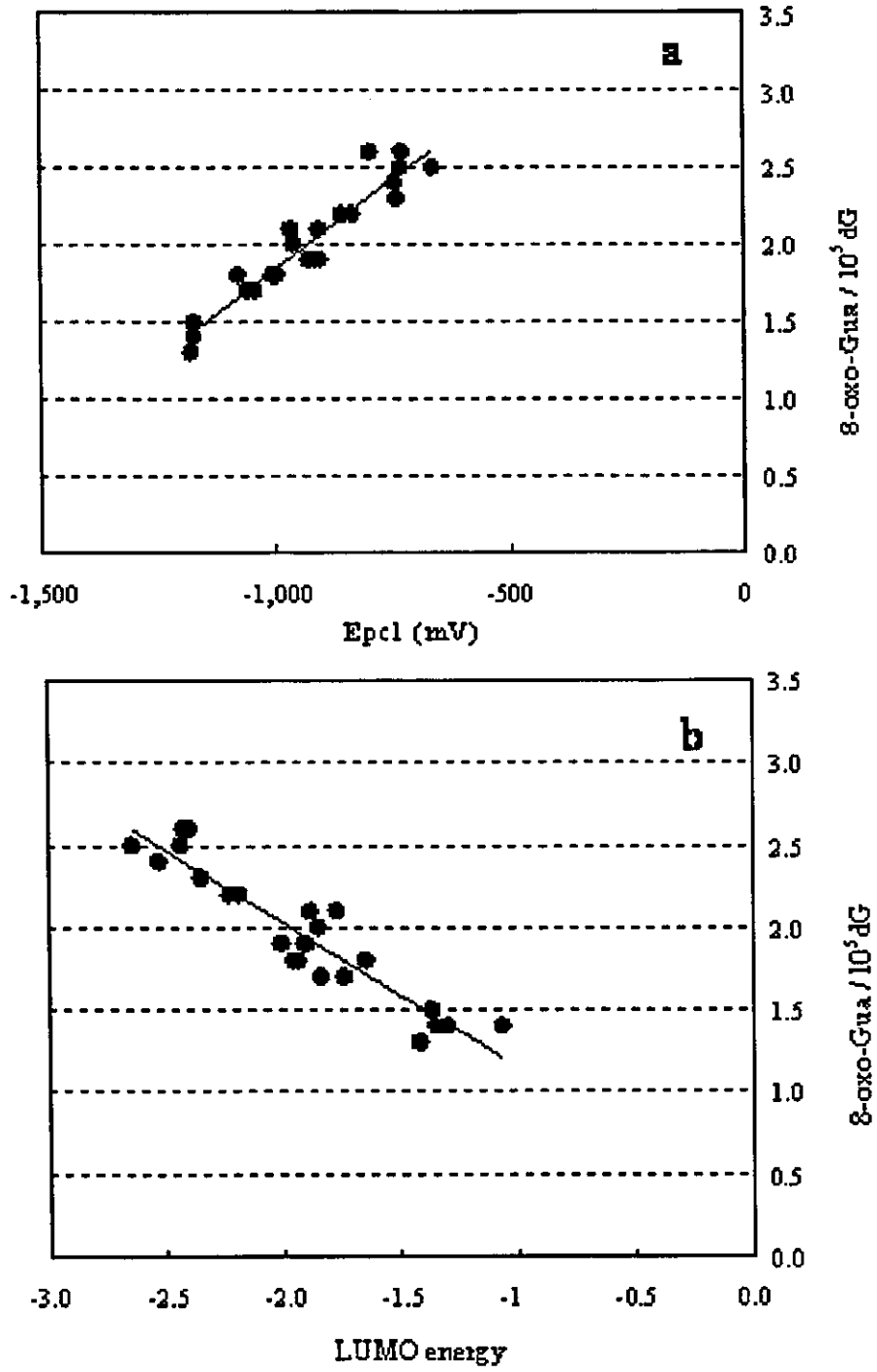

FIGURE 3. Correlation between 8-oxo-Gua formation, and the first reduction potentials (a), and LUMO energy (b) of NPhs. (a) $r = 0.906$; (b) $r = 0.874$.

of nitro substituents of aromatic rings and LUMO energy levels (9, 11). In fact, some derivatives substituted at positions 4 and 5 in the phenanthrene rings were perpendicular or almost perpendicular, and they were weak mutagens or nonmutagens. In contrast, those substituted on

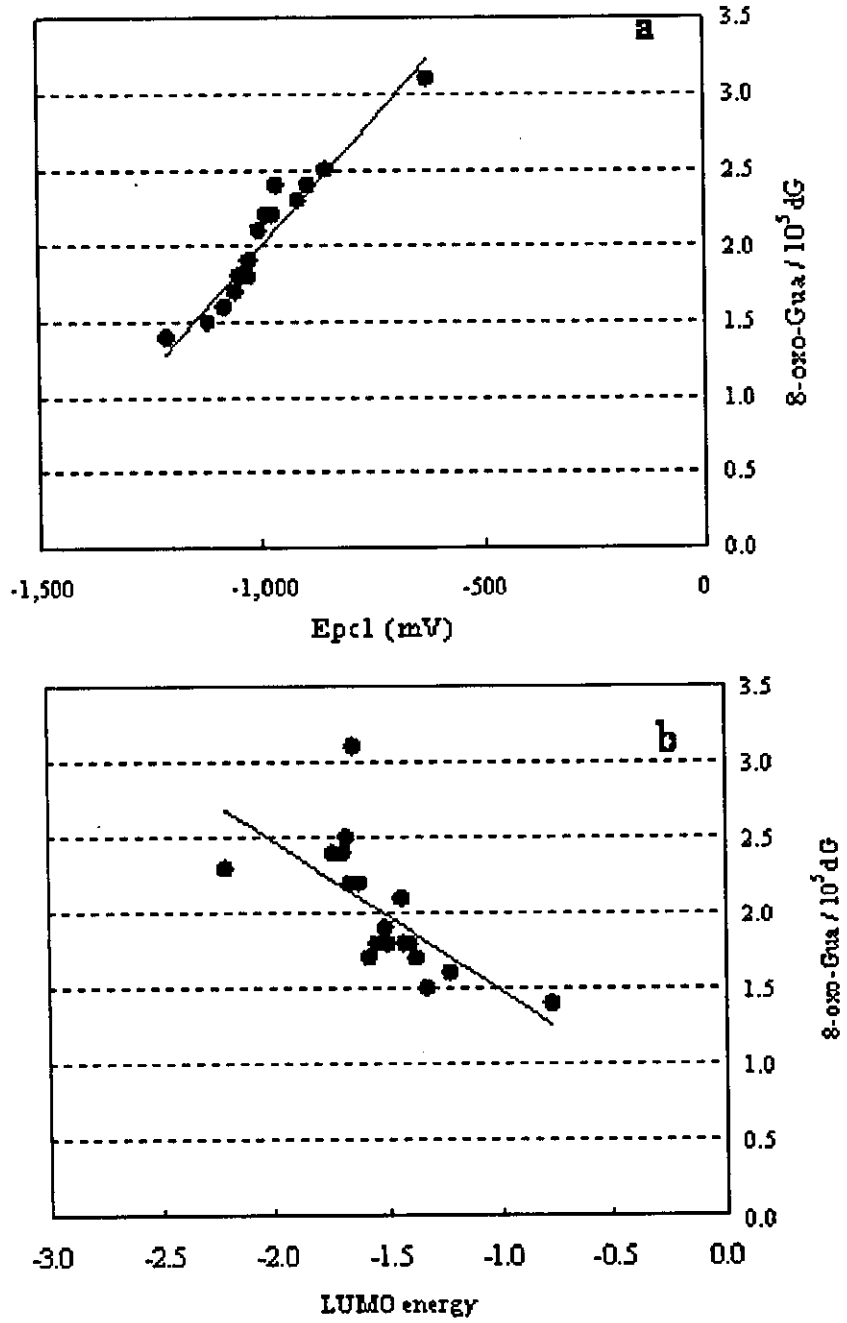

FIGURE 4. Correlation between 8-oxo-Gua formation, and the first reduction potentials (a) and LUMO energy (b) of NAPhs. (a) $r = 0.924$; (b) $r = 0.428$.

positions 2, 3, 6, and 7 were almost coplanar to the phenanthrene rings and were potent mutagens. NPhs substituted on positions 1, 8, 9, and 10 were noncoplanar because of steric hindrance of the aromatic proton at the peri position, with dihedral angles varying from 10° to 65°.

On the other hand, 8-oxo-Gua formed on the guanine residue on DNA is well known as cause of oxidative damage due to environmental

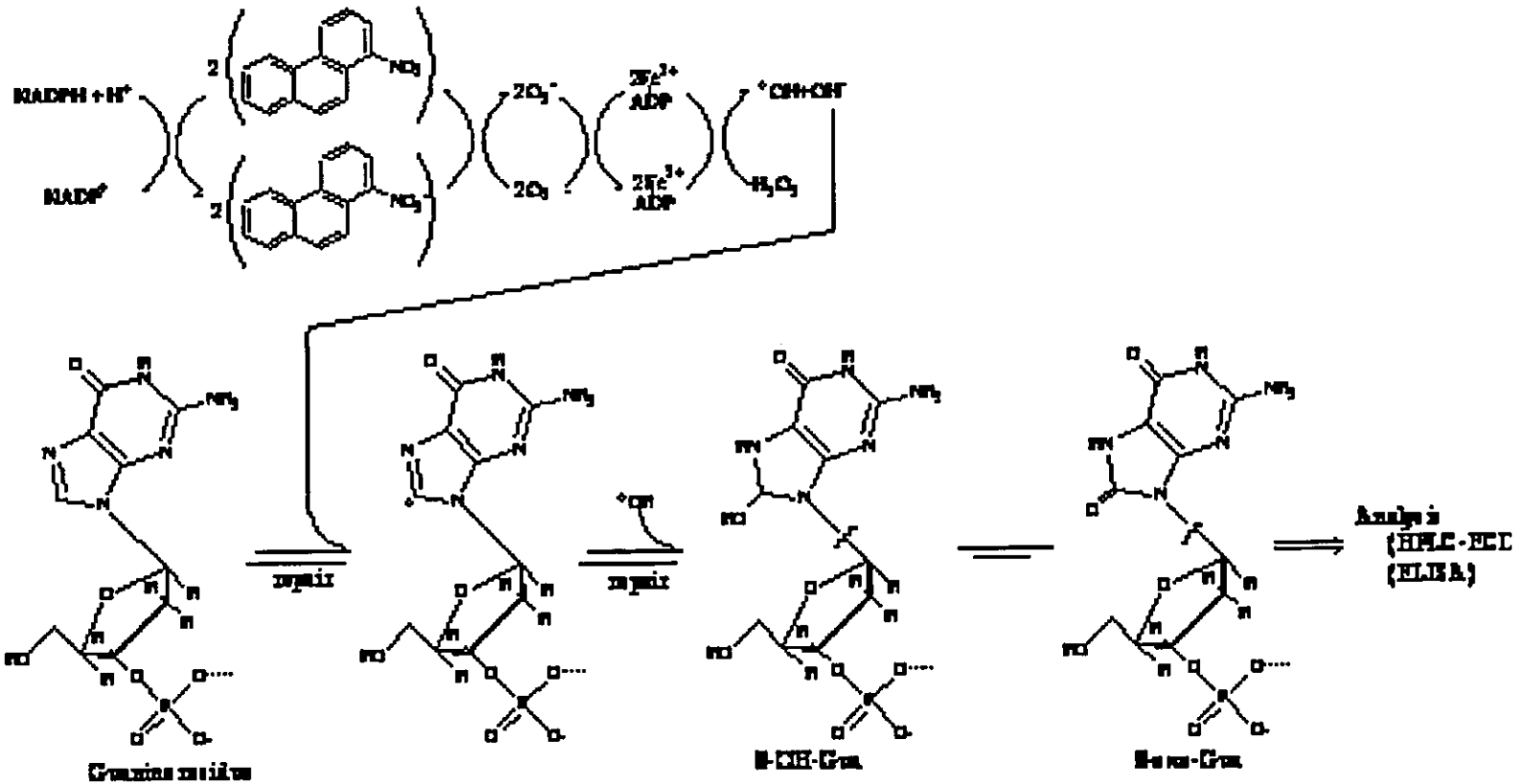

FIGURE 5. Possible mechanisms of oxidative damage in primary rat hepatocytes.

chemicals (18). By using primary rat hepatocytes, 8-oxo-Gua was effectively caused oxidative damage by generation of oxygen and hydroxyl radicals that were induced by nitro groups of NPhs and NAPhs. Thus, 8-oxo-Gua was effectively detected in primary rat hepatocytes by treatment with NPhs and NAPhs, and the induction was closely correlated with their chemical features; primary rat hepatocytes prepared in our laboratory effectively activated these derivatives, suggesting that cytochrome p450 in primary rat hepatocytes has sufficient enzymes to form 8-oxo-Gua. Primary rat hepatocytes showed growth regulation at the beginning of carcinogenesis (19), and in this study, 8-oxo-Gua formation by treatment of 4-NQO, a carcinogen, was observed with dose dependency (Figure 2). Similarly, 8-oxo-Gua formation by treatment with NPhs and NAPhs was significantly correlated with the first reduction potentials, and with LUMO energy for NPhs but not NAPhs. This was due to the fact that nitro groups of NPhs and NAPhs generated OH radicals in the metabolic pathway by microsome enzymes, and radical anions occurred at the 8-position of the guanine residue involving hydroxyl radicals in the presence of heme iron. This suggested that the formation of 8-oxo-Gua was promoted by primary rat hepatocytes. This was roughly the same as the results of many investigators who found increasing 8-oxo-Gua in peripheral lung tissue (17, 20–22).

It was reported that carboxylic acid derivatives of NPhs might induce multiple tumors in aristolochic acid (a herbal drug) patients (23). It was found that induction of mutagens and carcinogens caused the formation of a cyclic nitrenium ion with a decolorized charge by metabolic activation in microsomal enzymes (24–25). NPh derivatives are ubiquitous mutagens in environmental materials, but no NPhs or NAPhs have been detected in plant extracts.

REFERENCES

1. P. P. Fu, M. W. Chou, D. W. Miller, G. L. White, R. H. Heflich, and F. A. Beland, The Orientation of the Nitro Substituent Predicts the Direct-Acting Bacterial Mutagenicity of Nitrated Polycyclic Aromatic Hydrocarbons, *Mutation Res.* 143 (1985):173–181.
2. P. P. Fu, Y.-M. Zhang, R. H. Heflich, Y.-K. Wang, and J.-S. Lai, Effect of the Orientation of Nitro Substituent on the Bacterial Mutagenicity of Dinitrobenzo[*e*]pyrenes, *Mutation Res.* 225 (1989):1211–1225.
3. P. P. Fu, H. Jung, L. S. Von Tungeln, and R. H. Heflich, Mutagenicity of Mononitrodihydrobenzo[*a*]pyrenes, *Mutation Res.* 245 (1990):277–285.
4. H. Jung, A. U. Shaikh, R. H. Heflich, and P. P. Fu, Nitro Group Orientation, Reduction Potential, and Direct-Acting Mutagenicity of Nitro-Polycyclic Aromatic Hydrocarbons, *Environ. Mol. Mutagen.* 17 (1991):169–180.

5. G. Klopman and H. S. Rosenkranz, Structural Requirements for the Mutagenicity of Environmental Nitroarenes, *Mutation Res.* 126 (1984):227–238.
6. H. S. Rosenkranz, C. S. Michell, and G. Klopman, Artificial Intelligence and Bayesian Decision Theory in the Prediction of Chemical Carcinogens, *Mutation Res.* 150 (1985):1–11.
7. W. A. Vance and D. E. Levin, Structural Features of Nitroaromatics that Determine Mutagenic Activity in *Salmonella typhimurium*, *Environ. Mutagen.* 6 (1984):797–811.
8. T. Hirayama, T. Watanabe, M. Akita, S. Shimomura, Y. Fujioka, S. Ozasa, and S. Fukui, Relationships Between Structure of Nitrated Arenes and Their Mutagenicity in *Salmonella typhimurium*; 2- and 2,7-Nitro Substituted Fluorene, Phenanthrene and Pyrene, *Mutation Res.* 209 (1988):67–74.
9. N. Sera, K. Fukuhara, N. Miyata, and H. Tokiwa, Mutagenicity of Nitrophenanthrene Derivatives for *Salmonella typhimurium*: Effects of Nitroreductase and Acetyltransferase, *Mutation Res.* 349 (1996):137–144.
10. H. Tokiwa and Y. Ohnishi, Mutagenicity and Carcinogenicity of Nitroarenes and Their Sources in the Environment, *CRC Crit. Rev. Toxicol.* 17 (1986):23–60.
11. H. Tokiwa, N. Sera, K. Fukuhara, H. Utsumi, S. Sasaki, and N. Miyata, Structural Activity Relationship Between *Salmonella*-Mutagenicity and Nitro-Orientation of Nitroazaphenanthrenes, *Chemico-Biol. Interact.* 146 (2003):19–23.
12. M. Inoue, T. Osaki, M. Noguchi, S. Hirohashi, K. Yasumoto, and H. Kasai, Lung Cancer Patients Have Increased 8-Hydroxydeoxyguanosine Levels in Peripheral Lung Tissue DNA, *Jpn. J. Cancer Res.* 89 (1998):691–695.
13. H. Tokiwa, N. Sera, Y. Nakanishi, and M. Sagai, 8-Hydroxyguanosine formed in Human Lung Tissues and the Association with Diesel Exhaust Particles, *Free Radic. Biol. Med.* 27 (1999):1251–1258.
14. M. Nakajima, T. Takeuchi, and K. Morimoto, Determination of 8-Hydroxydeoxyguanosine in Human Cells under Oxygen-Free Conditions, *Carcinogenesis* 17 (1996):787–791.
15. H. Kasai, N. Iwamoto-Tanaka, T. Miyata, K. Kawanami, S. Kawanami, R. Kido, and M. Ikeda, Lifestyle and Urinary 8-Hydroxydeoxyguanosine, a Marker of Oxidative DNA Damage: Effects of Exercise, Working Conditions, Meat Intake, Body Mass Index, and Smoking, *Jpn. J. Cancer Res.* 92 (2001): 9–15.
16. H. Tokiwa, N. Sera, Y. Nakanishi, and M. Sagai, Formation of 8-Hydroxyguanosine by Purified Lung Particles and Involvement of Alveolar Macrophages, *Chemico-Biol. Interact.* (in press).
17. K. Fukuhara, M. Takei, H. Kageyama, and N. Miyata, Di- and Trinitrophenanthrenes: Synthesis, Separation, and Reduction Property, *Chem. Res. Toxicol.* 8 (1995):47–54.
18. S. Shibutani, M. Takeshita, and A. P. Grollman, Insertion of Specific Bases During DNA Synthesis Past the Oxidation-Damaged Base 8-oxodG, *Nature* 349 (1991): 431–434.
19. A. Low-Baselli, K. Hufnagl, W. Parzefall, P. Schulte-Hermann, and B. Grasl-Kranpp, Initiated Rat Hepatocytes in Primary Culture: A Novel Tool to Study Alterations in Growth Control During The First Stage of Carcinogenesis, *Carcinogenesis* 21 (2000):79–86.

20. M. Lodovici, C. Casalini, R. Cariaggi, L. Michelucci, and P. Dolara, Levels of 8-Hydroxydeoxyguanosine as a Marker of DNA Damage in Human Leukocytes, *Free Radic. Biol. Med.* 28 (2000):13–17.
21. M. Nagashima, H. Kasai, J. Yokota, Y. Nagamachi, T. Ichinose, and M. Sagai, Formation of an Oxidative DNA Damage, 8-Hydroxydeoxyguanosine, in Mouse Lung DNA after Intratracheal Instillation of Diesel Exhaust Particles and Effects of High Dietary Fat and Beta-Carotene on this Process, *Carcinogenesis* 16 (1995):1441–1445.
22. H. Tokiwa, N. Sera, K. Horikawa, Y. Nakanishi, and N. Shigematu, The Presence of Mutagens/carcinogens in the Excised Lung and Analysis of Lung Cancer Induction, *Carcinogenesis* 14 (1993):1933–1938.
23. V. M. Arlt, M. Stiborova, and H. H. Schmeiser, Aristolochic Acid as a Probable Human Cancer Hazard in Herbal Remedies: A Review, *Mutagenesis* 17 (2002):265–277.
24. H. H. Schmeiser, C. A. Bieler, M. Wiessler, C. van Ypersele de Strihou, and J. P. Cosyns, Detection of DNA Adducts Formed by Aristolochic Acid in Renal Tissue from Patients with Chinese Herbs Nephropathy, *Cancer Res.* 56 (1996):2025–2028.
25. H. Schmeiser, E. Frei, M. Wiessler, and M. Stiborova, Comparison of DNA Adduct Formation by Aristolochic Acids in Various in Vitro Activation Systems by 32P-Post-labelling: Evidence for Reductive Activation by Peroxidases, *Carcinogenesis* 18 (1997):1055–1062.

Bull.Natl.Inst.Health Sci., **122**, 10-15 (2004)　**Originals**

芳香族 *N*-ニトロソ化合物の NO 遊離能と DNA 切断活性

NO-Release Ability and DNA-Damage Activity of Aromatic *N*-Nitroso Compounds

丹野雅幸*・末吉祥子・福原　潔・宮田直樹*・奥田晴宏

Masayuki Tanno*, Shoko Sueyoshi, Kiyoshi Fukuhara, Naoki Miyata*, Haruhiro Okuda

To develop a new nitric oxide-donor (NO-donor) that is useful for chemical and biochemical research, we synthesized several aromatic *N*-nitroso compounds including 1-[*N*-nitroso-*N*-(4-tolyl)carbamoyl] piperidine-4-carboxylic acid (**1f**) and phenyl(2-pyridyl)-*N*-nitrosamines, which spontaneously generate NO at ambient temperature. Thermal decomposition of these compounds was run under mild conditions. Gaseous NO released from them was quantified by means of the Griess reaction using a specially designed apparatus in which NO_2^- is generated from NO. The structure of products arose from the radical cleavage of N-NO bond was clarified by chemical and spectral studies. Generation of NO from the *N*-nitroso compounds was also confirmed by ESR spectroscopy. The action of these NO-releasing compounds against DNA was examined. When the pBR 322 DNA was treated with **1f** at 37 °C for 3 h, the DNA single-strand breaks was 31 % for 1 mM of **1f**. The denitrosated compound and sodium nitrite did not show any effective DNA-cleaving activity. On the other hand, aromatic *N*-nitrosamines induced weak DNA-cleaving activity under the same condition.

Keywords: NO-donor, *N*-nitrosourea, phenylpyridyl-*N*-nitrosamine, DNA-cleaving activity

緒　言

N-ニトロソ化合物の N-NO 結合は酸触媒下ではイオン的に容易に切断されるが，中性条件下では光や高温加熱によりラジカル的に切断されることが知られている.[1] 我々は最近，Fig.1 に示すような芳香環を持つ *N*-ニトロソ化合物（1－4）（1e, 3c, 4d を除く）が中性条件下室温でもラジカル的に N-NO 結合の解裂を起こし，一酸化窒素（NO）を遊離することを見い出した．それに対し脂肪族 *N*-ニトロソ化合物（5，6）は同一条件下ではラジカル解裂しないことを明らかにした.[2] さらに，芳香環を持つ *N*-ニトロソ化合物の N-NO 結合が温和な条件下で NO を与えるようにラジカル解裂しやすい原因は，*N*-ニトロソ化合物のコンホメーションに起因することを明らかにした.[3]

本論文では生物学及び化学的に有用な NO ドナーを開発する目的で水溶性芳香族 *N*-ニトロソ尿素類（1f）や複素環 *N*-ニトロソアミン類（4f-k）を合成し，その分解反応を検討すると共に，これらの *N*-ニトロソ化合物の NO 発生能とプラスミド DNA に対する作用を調べた．

* To whom correspondence should be addressed:
Masayuki Tanno; Kamiyoga 1-18-1, Setagaya, Tokyo, 158-8501, Japan; Tel: 03-3700-1141 ext. 223;
E-mail: tanno@nihs.go.jp
*Faculty of Pharmaceutical Sciences, Nagoya City University, 3-1 Tanabetori, Mizuho-ku, Nagoya-shi, 467-0027 Japan

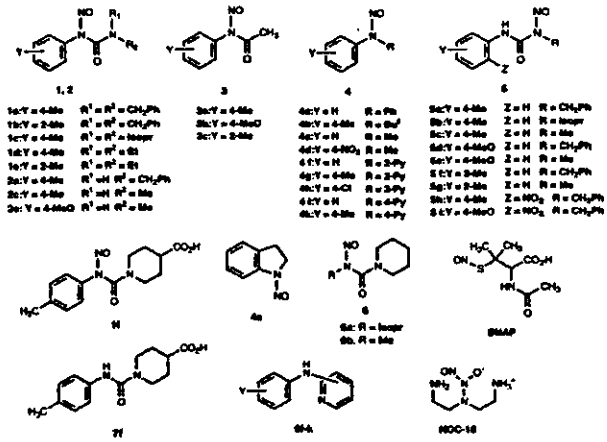

Fig.1 Structure of *N*-nitroso derivatives and rerated compounds

実験方法

1．芳香族尿素（7f）の合成

クロロホルム（$CHCl_3$）（70 ml）とジメチルスルホキシド（DMSO）（10 ml）の混合溶媒にイソニペコチン酸（2.0 g, 16 mmol）を溶解し，4－トリルイソシアナート（2.4 g, 18 mmol）を徐々に加え，さらに，クロロホルムを加えて溶媒の全量を 90 ml とし，室温で 5 日間撹拌．反応液は黄色透明になる．TLC（シリカゲル薄層板，展開溶媒はクロロホルム）で原料が残っているかどうかを確認．残っていれ

ばさらに撹拌を続ける．生じた白色の固体をろ過して採取．得られた白色の固体をクロロホルムに溶解し，不溶物のジトリル尿素をろ過して除き，溶解物をクロロホルムで再結晶して針状晶の7fを得た．融点130-131℃，収率は27 %．スペクトルデータをTable 1に示した．

2．複素環アミン類（8 f-k）の合成

典型例として化合物（8f）について示す．複素環アミン（8f）の合成：アニリン（2.8 g，3 mmol）に2-クロロピリジン（3.4 g，3mmol）を加え，150℃，3時間熱した．反応後，氷水を加え，炭酸水素ナトリウムでアルカリにする．エーテルで抽出．無水硫酸ナトリウムでエーテル溶媒を乾燥後，ろ過し，エーテル溶媒を減圧濃縮して褐色の固体アミン（8f）を98 %の収率で得た．他の複素環アミン類（8g-k）も同様にして得た．NMRスペクトルデータをTable 1に示す．なお，これらの化合物を得る際の抽出溶媒にはジクロロメタンを用いた．

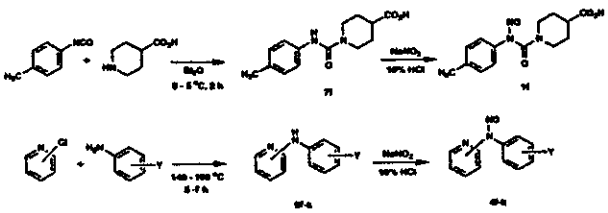

Fig.2 Syntheses of aromatic *N*-nitrosourea (1f) and *N*-nitrosoamines (4f-k)

3．NOを遊離する*N*-ニトロソ化合物(1f, 4f-k)の合成

典型例として1-[*N*-ニトロソ-*N*-(4-トリル)カルバモイル]ピペリジン-4-カルボン酸（1f）とフェニル(2-ピリジル)-*N*-ニトロソアミン（4f）について示す（Fig. 2）．化合物1fの合成:芳香族尿素（7f）(1.02 g，3.9 mmol)を99 %ギ酸5 mlに溶解させ5℃以下で，激しく撹拌しながら亜硝酸ナトリウム（0.56 g，8.0 mmol）を約20分間かけて徐々に加えると，反応液は黄色になった．これを30分間冷却下で反応させた後，氷片を加えると橙色油状物が生じた．この油状物を冷クロロホルムで抽出し，氷水で洗浄水が酸性を呈さなくなるまで洗浄した．冷クロロホルム層をシリコン処理ろ紙（silicone-treated filter paper（1 ps phase separators, Whatman Ltd.））でろ過し，ろ液は冷却下で減圧濃縮した．収率は58.6 %．冷凍庫に保存．

化合物4fの合成：複素環アミン(8f)（0.31 g，2.0 mmol）を20 %塩酸（15ml）に溶解した後，冷却下で水（10 ml）に溶かした亜硝酸ナトリウム（170 mg，2.5 mmol）溶液を加え，0℃下で撹拌し，30分間，反応させた．冷水を加えた後，炭酸水素ナトリウムで中和し，冷時ジクロロメタンで抽出した．冷ジクロロメタン層をシリコン処理ろ紙（silicone-treated filter paper（1 ps phase separators, Whatman Ltd.））でろ過し，ろ液は冷却下で減圧濃縮した．残留物は冷エーテルで再結晶．他のニトロソアミン類（4g-k）も同様にして得た．NMRスペクトルデータをTable 1に示した．なお，^{13}C-NMRは室温で測定したが，4f-kは速やかに操作することによりデータが得られた．しかし，1fの場合は測定中に一部分解が認められた．

4．化合物1fと4fの分解反応と分解生成物の別途合成

化合物1fの分解反応：1f（0.73 g，2.5 mmol）をクロロホルム（100 ml）に溶かし，37℃で3時間放置させた後，生じたN-NO解裂由来[1]の各分解生成物（7f，11f）をカラムクロマトグラフィーで精製した．この時，N-NO解裂由来以外の生成物である副生物トリアゼン[4]の単離精製は行わなかった．各分解生成物の構造はFig.3に示した経路から別途に合成し，融点，NMRスペクトルデータから決定した（Table 1）．

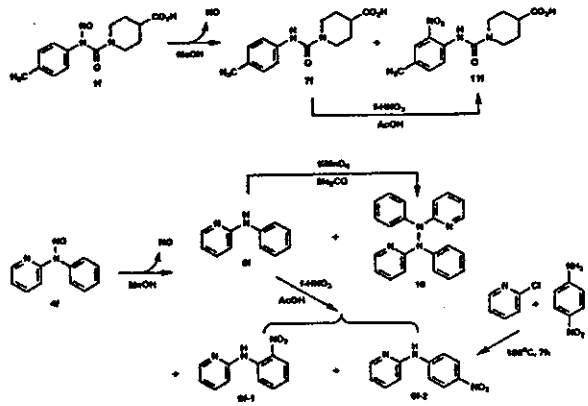

Fig.3 Decomposition of *N*-nitrosourea (1f) and *N*-nitrosamine (4f)

11fの別合成：尿素7f（0.65 g，2.4 mmol）を酢酸（10 ml）に溶解し，撹拌しながら15℃以下に保つように冷却して，発煙硝酸（0.6 ml）を少量ずつ滴下していくと，黄色溶液になる．約1時間撹拌し，反応混合液を氷の中へ少量ずつ注ぎ込むと，白黄色油状物質が析出してくる．これをクロロホルムで抽出し，水槽が酸性を示さなくなるまでクロロホルムを水で洗った．このクロロホルム層を無水硫酸ナトリウムで乾燥後，溶媒を留去すると，黄色の結晶（融点156-157℃）の11fが0.56 g（収率73.9 %）得られた．

4fの分解反応：化合物（4f）(0.80 g，4.0 mmol）を有機溶媒（メタノール又はクロロホルム）（50 ml）に溶かし，37℃で5時間放置させた．この時，出発原料の*N*-ニトロソ体の分解率は4 %であった．発生するNO以外の分解生成物は展開溶媒（n-ヘキサン：エーテル：クロロホルム＝5:4：1）を用いてTLC（シリカゲル）を行うと，9f-1，4fと10，8f，9f-2の順で展開された．これらの分解生成物の構造はFig. 3に示した経路から別途に合成し，融点及びNMRスペクトルデータから決定した（Table 1）．

8fから9f-1と9f-2の合成：8f（0.85 g，5.0 mol）

を酢酸(10ml) に溶解し，撹拌しながら 15°C 以下に保つように冷却して，発煙硝酸 (0.6 ml) を少量ずつ滴下していくと，黄色溶液になる．約1時間撹拌し，反応混合液を氷の中へ少量ずつ注ぎ込むと，油状物質が析出した．これをクロロホルムで抽出し，水槽が酸性を示さなくなるまでクロロホルム層を水で洗った．このクロロホルム層を無水硫酸ナトリウムで乾燥後，溶媒を留去すると，9f-1 と 9f-2 の混合物が得られた．この混合物を少量のクロロホルムに溶かし，シリカゲルカラムクロマトグラフィーで精製した．クロロホルムとエーテルの混液 (8 : 2) を展開溶媒とした．最初のフラクションから 9f-1 (融点66-67°C，収率3.0 %) が得られた．次に 9f-2 (融点66-67°C，収率36.0 %) が得られた．NMRスペクトルデータをTable 1に示す．さらに，9f-2は2-クロロピリジンと4-ニトロアニリンを反応させても得られた． 2-クロロピリジン (2.3 g, 20 mmol) と4-ニトロアニリン (2.7 g, 20 mmol) を混合し，150°C，7時間撹拌しながら反応させた．反応後，氷水を加え，炭酸水素ナトリウムでアルカリにする．クロロホルムで抽出．無水硫酸ナトリウムでクロロホルム層を乾燥後，ろ過し，クロロホルム溶媒を減圧濃縮して黄色のニトロ体 9f-2 を79 % の収率で得た．

ヒドラジノ誘導体 (10) の別途合成[5] ： 過マンガン酸カリ (79 mg, 5 mmol) のアセトン (10 ml) 溶液に 8f (0.26 g, 1.5 mmol) と硫酸ナトリウム (0.5 g) のアセトン (10 ml) 溶液を0°Cで加えて，一夜撹拌した．ろ過してアセトンを留去し，残留物をシリカゲルカラムクロマトグラフィーで精製した．最初のフラクションは原料の 8f，次に化合物 (10) を得た (分解点 182°C 収率 9.0 %)．NMR スペクトルデータを Table 1 に示した．

5．遊離 NO の確認と発生能の測定

一定量の *N*-ニトロソ化合物が一定温度下で，一定時間内に分解して発生する NO 量の測定は，我々が考案した簡易型装置[3]を用いて行った．*N*-ニトロソ化合物 (1 x 10^{-3} mol) を有機溶媒 ($CHCl_3$)(2 ml) または緩衝液(Krebs buffer: pH 7.4) に溶解し，37°C で 2 時間加温した．発生するガスを捕集し，NO_2^-に変えて呈色させた．呈色試薬としてグリース試薬 (4-アミノベンゼンスルホン酸および *N*-ナフチルエチレンジアミンの希酢酸溶液) (2ml) を使用した．2 時間反応後，546 nm における吸光度を測定し，亜硝酸ナトリウム標準液を用いて作成した検量線から NO_2^-の量を算出した．結果を Table 2 に示した．

6．ESR 装置による NO の確認

2-(4-カルボキシフェニル)-4,4,5,5-テトラメチルイミダゾリン-1-オキシル 3-オキシドのナトリウム塩 (Carboxy-PTIO) および *N*-(ジチオカルバモイル)-*N*-メチル-D-グルカミンのナトリウム塩-二価イオン鉄錯体 (MGD-Fe^{2+} 錯体) をNO検出試薬として使用して日本電子製JES-FA100で電子共鳴スピン ESR (x-band ESR) を測定した．MGD-Fe^{2+}

Table 1 ^{13}C-NMR Chemical shift (ppm) of *N*-nitroso compounds (1, 4) and related compounds [a]

Compd.	Y-Ph-N(X)-Z			Phenyl						Pyridyl (or Piperidyl)					Me	CO
No.	X	Y	Z	C-1	C-2	C-3	C-4	C-5	C-6	C-2	C-3	C-4	C-5	C-6		
4f	NO	H	2-Py	135.42	127.89	129.55	129.55	129.55	127.89	155.31	121.72	138.45	113.45	148.52		
8f	H	H	2-Py	140.62	120.49	129.25	122.74	129.55	120.49	156.29	108.08	137.70	114.79	148.27		
4g	NO	4-Me	2-Py	132.67	127.58	130.31	139.70	130.31	127.58	155.43	138.40	137.64	113.39	148.53	21.39	
8g	H	4-Me	2-Py	132.72	121.28	129.81	137.04	129.81	121.28	156.71	137.64	149.92	114.46	148.34	20.82	
4h	NO	4-Cl	2-Py	135.50	129.13	129.83	133.59	129.83	129.13	155.04	121.85	138.56	113.33	148.46		
8h	H	4-Cl	2-Py	139.23	121.32	129.32	129.10	129.32	121.32	155.75	108.54	137.86	115.23	148.25		
4i	NO	H	4-Py	134.47	127.86	130.37	130.53	130.37	127.86	149.83	111.73	149.92	149.92	111.73		
8i	H	H	4-Py	139.60	121.61	129.54	124.09	129.54	121.61	150.72	109.46	150.16	150.16	109.46		
4k	NO	4-Me	4-Py	131.97	127.51	130.89	140.68	130.89	127.51	149.26	111.67	150.55	150.55	111.67	21.32	
8k	H	4-Me	4-Py	134.36	122.46	130.15	136.59	130.15	122.46	151.74	109.08	149.18	149.18	109.08	21.90	
9f-1	H	2-NO_2	2-Py	129.30	138.97	126.24	119.69[b]	135.70	119.59[b]	153.61	113.83	138.06	117.86	147.96		
9f-3	H	3-NO_2	2-Py	142.08	116.40	148.90	116.29	129.73	124.44	154.66	110.06	138.06	113.12	148.12		
9f-2[c]	H)	4-NO_2	2-Py	147.34	116.53	125.19	139.89	125.19	116.53	154.58	112.36	137.53	116.44	147.34		
10	[d]			141.78	120.17	128.81	123.66	128.81	120.17	156.16	110.57	138.24	116.99	147.88		
1f[e]	NO	4-Me	[f]	132.95 136.29	120.47 125.34	129.46 130.28	137.05	129.46 130.28	120.47 125.34	43.70	27.49[g]	39.98	27.49[g]	43.70	20.73 21.09	155.58, -
7f	H	4-Me	[f]	130.42	119.92	128.53	137.96	128.53	119.92	43.26	27.89	40.37	27.89	43.26	20.32	155.08, 175.67
11f	H	4-Me-2-NO_2	[f]	131.50	135.05	125.32	135.56	137.05	121.53	43.61	27.90	40.85	27.90	43.61	20.37	153.65, 174.05

[a] Measured in $CDCl_3$ with TMS as an internal standard. Ph=phenyl, Py=pyridyl [b] Data in DMSO-d_6 [c] Ph(2-Py)N-NPh(2-Py) [d] Z=$CO(CH_2)_5CO_2H$ [e] Decomposed during the measurement. [f] Assignments may be reversed. [g] Coincidences

Table 2　NO-Releasing ability of various *N*-nitroso compounds [a]

Compd.	Y-Ph-N(NO)-X [b] Y	X	mM
1a	4-Me	$CON(Bn)_2$	4.79
1a	4-Me	$CON(Bn)_2$	0.45 [f]
1f	4-Me	$CON(CH_2)_5CO_2H$	2.04
1f	4-Me	$CON(CH_2)_5CO_2H$	0.04 [e]
4a	H	Ph	0.02 [d]
4f	H	2-Py	0.52 [c]
4g	4-Me	2-Py	0.46 [c]
4h	4-Cl	2-Py	0.52 [c]
4i	H	4-Py	0.52 [c]
4k	4-Me	4-Py	0.26 [c]
NOC-18			0.46 [e]
SNAP			0.55
SNAP			0.50 [f]

[a] Concentration of each *N*-nitroso compound and SNAP for thermal decomposition in $CHCl_3$ was 1-10 x 10^{-3} M. Reactions were carried out at 37°C for 2h. Detection as NO_2^- using the Griess method. The values are amounts of NO_2^- generated via NO from the 100 mM $CHCl_3$ solution of the compound. b) Bn=benzyl, Ph=phenyl, Py=pyridyl. [c] Reacted for 4h. [d] Reacted for 7h. [e] Reacted in the Krebs buffer (pH 7.4). [f] Reacted in the mixture of DMSO-Krebs buffer (1:9).

錯体はアルゴン置換した塩化第一鉄（$FeCl_2$）(3mM) とMGD (5mM) の水溶液を測定直前に混合して作成した．Carboxy-PTIOによる検出は5 μM Carboxy-PTIOと20 μM 化合物のジメチルホルムアミド（DMF）と蒸留水 の 1：4 溶液を調整して行った．MGD-Fe^{2+}錯体による検出は，MGD-Fe^{2+}錯体と200 μM 化合物のDMSOとpH 7.2リン酸緩衝液の1：4 溶液を調整して行った．結果をFig.4に示した．

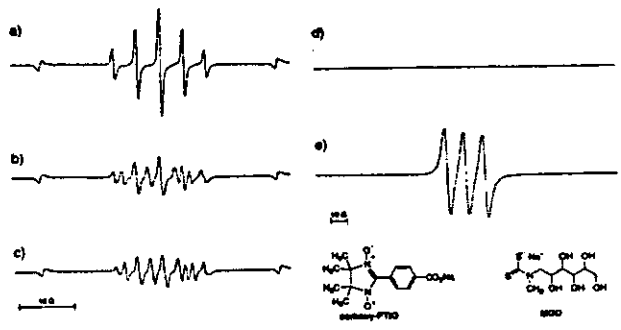

Fig.4 ESR spectra of variable PTIO dervatives MGD with NO produced from *N*-nitrosamine (4f)

a) 5 μM of carboxy-PTIO in H_2O ;b) 5 μM of carboxy-PTIO and 20 μM of 4f in a mixture of DMF and H_2O (1:4) ;c) after 20 sec.;d)15mM of MGD and 3 mM of $FeCl_2$ in a mixture of DMSO and phosphate buffer,pH 7.2 (1:4) ;e) 200 μM of 4f,5mM of MGD and 3mM of $FeCl_2$ in a mixture of DMSO and phosphate buffer,pH 7.2 (1:4)

7．DNA切断活性

芳香族*N*-ニトロソ尿素（1f），*N*-ニトロソアミン（4a, 4f-i）および1-ヒドロキシ-2-オキソ-3,3-ビス(2-アミノエチル)トリアゼン（NOC-18）についてDNA切断活性を測定した．化合物をDMFとTris-HCl-buffer（pH 7.2）の混液（1：4）に溶解し，調製したpBR 322プラスミドDNAを加えて37°Cで3時間振盪した後，アガロース電気泳動（70 V，2時間）を行った．泳動帯の量比を画像解析（NIH-Image）により算出した．結果をTable 3および4に示した．

Table 3　DNA-Cleaving activity of various *N*-nitroso compounds [a]

Compd.	mM	DNA Cleavage Form I (%)	Form II (%)
1f	1	67	33
1f	10	31	69
4f	1	96	4
4f	10	93	7
7f	1	97	3
7f	10	95	4
8f	1	98	2
8f	10	95	5
NOC-18	1	69	31
NOC-18	10	60	40
$NaNO_2$	1	96	4
$NaNO_2$	10	96	4

[a] Treated for 3 h

Table 4　DNA-Cleaving activity of aromatic *N*-nitrosamines [a]

Compd.	mM	DNA Cleavage Form I (%)	Form II (%)
4a	10	97	3
4f	10	95	5
4g	10	88	12
4h	10	93	7
4i	10	80	20
$NaNO_2$	10	97	3

a) Treated for 3 h

結果及び考察

N-ニトロソ化合物（1f，4f-k）はFig.2に示したように合成した．*N*-ニトロソ尿素誘導体（1f）の場合はアリールイソシアナートにイソニペコチン酸を反応させて得た尿素誘導体（7f）をニトロソ化して合成した．また，複素環

N-ニトロソアニリン類 (4) はアニリン誘導体にハロゲノピリジン類を加熱反応して得たアミン類 (8) を酸性下に亜硝酸ナトリウムでニトロソ化して得た．次に，得られたN-ニトロソ体 (1f) を室温下及び種々の条件下で分解させた (Fig.3)．N-ニトロソ尿素 (1f) をクロロホルム中で分解させると，尿素誘導体の分解生成物 (7f, 11f) を生じた．また，ニトロ体 (11f) は別途合成として7fをニトロ化して得られた．これら尿素誘導体の構造はNMRスペクトルデータで確認した (Table 1)．一方，複素環N-ニトロソアニリン (4f) の分解は37℃, 5 時間で行った．この時，出発原料のN-ニトロソ体の分解率は4 % であった． Fig.3に示したように3種類のアリールアミン類 (8f, 9f-1, 9f-2) とテトラ置換ヒドラジン類 (10) が生成することがわかった．これらの生成物の構造は，また別ルートで合成を行い (Fig.3)，それら化合物の構造が間違いないことをスペクトルデータで確認した (Table 1)．なお，N-ニトロソ尿素体 (1f) や複素環N-ニトロソアニリン (4f) が分解の際に相当する2-ニトロ体や4-ニトロ体が生じることは (3-ニトロ体 (9f-3) の生成は認められなかった)，分解過程でNOの生成を示している．[3] そこで，これらの化合物からの単位時間あたりのNO発生量を調べた．合成したN-ニトロソ化合物を有機溶媒に溶かし，また，やや水溶性のある化合物はDMSO-Krebs緩衝液に，水溶性化合物はKrebs 緩衝液に溶かし，37℃でNOを発生させた．各種のN-ニトロソ化合物 (4f-k, 1f) (Fig.1) の NO発生能 (単位mmolと時間あたりに発生するNOの量) を既知のNO ドナーである S-ニトロソ-N-アセチル-DL-ペニシラミン (SNAP) や水溶性NOC-18と共にTable 2に示した．また，既にNO発生に関し，報告済みの化合物 (1a, 4a) もこの表に加え，比較検討した．芳香族N-ニトロソ化合物のNO発生能は，三置換尿素誘導体 (1a) が最も大きいが，今回合成した 1f は 1a の約半分の NO 発生能を示した．1a は，水に難溶であったが，1fはKrebs 緩衝液中NO発生能を調べることが可能になり，その結果NOC-18 の1/10 であることがわかった．また，ジアリールニトロソアミン (4) については，フェニル基をピリジル基にすることによって発生能が約 20 倍増加した (Table 2: 報告済み4a と今回合成した4f-i を比較)．なお，脂肪族N-ニトロソ化合物 (5, 6) からのNO発生は室温下では認められていない．[3] さらに，N-ニトロソ化合物 (1, 4) から NO が遊離していることの確認は，一酸化窒素のテトラフェニルポルフィリン錯体 (NO-TPP-Co(II) 錯体) の単離と Carboxy-PTIO および MGD-鉄錯体を用いたESR 測定法でも行った．即ち，ニトロソ化合物の添加により Carboxy-PTIO が 2-(4-カルボキシフェニル)-4, 4, 5, 5-テトラメチルイミダゾリン-1-オキシルのナトリウム塩 (Carboxy-PTI) へ変わるのに伴い経時的にESR スペクトルが変化した (Fig.4, a-c)．さらに，塩化第一鉄存在下で MGDと化合物の反応ではMGD-鉄錯体にNOが配位し，MGD-Fe-NO 錯体が生成し，特有のスペクトルを示した (Fig.4, d, e)．

一方，芳香族N-ニトロソ尿素 (1f)，N-ニトロソアミン (4a, 4f-i)，非ニトロソ体 (7f, 8f) およびNOC-18 について DNA 切断活性を測定した．化合物を DMF と Tris-HCl-buffer (pH 7.2) の混液 (1 : 4) に溶解し，調製したpBR 322 プラスミド DNA を加えて 37℃ で3時間振盪した後，アガロース電気泳動 (70 V, 2 時間) を行った．泳動帯の量比を画像解析により算出した．結果をTable 3 および4に示した．芳香族ニトロソ化合物，1f の DNA 切断活性を NOC-18 と比較すると，NOC-18 の一本鎖切断活性 (Form II の生成) は 1 mM で 31 %, 10 mM で 40 % であったのに対して，1f は一本鎖切断型 (Form II) が 1 mM で 33 %, 10 mM で 69 % 生成し，より強力な活性を示した (Table 3)．一方，脱ニトロソ体 (7f) や 亜硝酸ナトリウム ($NaNO_2$) では切断活性を示さず，また NO 生成能が低い芳香族ニトロソアミンの活性は非常に弱いことがわかった．この結果は，既に報告した細胞障害作用における活性とニトロソ体の NO 生成能が相関する[3] ことと一致し，1f による DNA 切断反応が化合物より生成した NO または NO 由来の活性種に起因していることを示唆している．NOC-18のNO生成能は1fより大きいにもかかわらず活性が低いのは，1f に比べて分解速度が速いのでNOC-18から遊離したNO が DNA に化学的に付加反応を起こす前にDNA以外へ物理的に拡散してしまい効率よくDNAに作用しない可能性と芳香環を持つ 1f の方がDNA に対する親和性が高いこと等の影響によると推定した．一方，芳香族ニトロソアミンから生ずる NO による生物作用の報告は無い．ピリジルフェニルニトロソアミン類 (4f-i) は芳香族N-ニトロソ尿素 (1f) と比較すると活性は弱いが，その切断反応は有意に進行した (Table 4)．ピリジルフェニルニトロソアミン類 (4f-i) の DNA 切断活性はジフェニルニトロソアミン (4a) よりも大きく，NO 生成能の傾向とも一致した．したがって，これらの化合物についても芳香族ニトロソ尿素と同様にNOまたは NO 由来化合物が活性種である可能性を示している．さらに，4f-k は1fに比べ，分解速度は遅いが，徐放性を持つNOドナーの開発に発展する可能性を示すもので興味深い結果である．

文　献

1) a) S.S.Singer, W.Lijinsky,and G.M.Singer, *Tetrahedron Lett.*,1613-1616(1977);b)S.S.Singer,G.M.Singer, and B.B.Cole, *J.Org.Chem.*,45,4931-4935(1980);c)B.C. Challis and M.R.Osborne,*J.Chem.Soc.,Parkin II*,1973,1526-1533.d) J.N.Tam,R.W.Yip,and Y.L.Chow,*J.Amer. Chem.Soc.*,96,4543-4549(1974) ;e)R.H.Smith,Jr., M.B.Kroeger-Koepke,and C.J. Michejda,*J.Org.Chem.*,47,2907-2910(1982);f) P.Welzel,*Chem.Ber.*,104,808-821(1971);g)

A.J.Buglass,B.C.Challis and M.R.Osborne,*IARC Sci. Publ.*,**9**,94-100 (1974); h)R.S.Lowe,J.N.S.Tam,K.Hanaya,and Y.L.Chow,*J.Am.Chem.Soc.*,**97**,215-216 (1975)

2) a) S.Sueyoshi and M.Tanno, *Chem.Pharm.Bull.*,**33**, 488-496(1985);b)M.Tanno and S.Sueyoshi,*ibid.*,**35**,1360-1371(1987);c)M.Tanno,S.Sueyoshi,and S.Kamiya,*ibid.*,**38**, 49-54(1990);d)M.Tanno,S.Sueyoshi,and S.Kamiya,*ibid.*, **38**,2644-2649(1990)

3) M.Tanno,S.Sueyoshi,N.Miyata,and K.Umehara,*Chem. Pharm.Bull.*,**45**,595-598(1997)

4) M.Tanno,S.Sueyoshi,N.Miyata,and S.Nakagawa,*Chem. Pharm.Bull.*,**44**,1849-1852(1996)

5) F.A.Neugebauer and P.H.H.Fischer,*Chem.Ber.*,**98**,844-850(1965)

ARTICLE

OBC
www.rsc.org/obc

Electron-transfer mechanism in radical-scavenging reactions by a vitamin E model in a protic medium

Ikuo Nakanishi,*[a,b] Tomonori Kawashima,[a,c] Kei Ohkubo,[b] Hideko Kanazawa,[c] Keiko Inami,[d] Masataka Mochizuki,[d] Kiyoshi Fukuhara,[e] Haruhiro Okuda,[e] Toshihiko Ozawa,[a] Shinobu Itoh,[f] Shunichi Fukuzumi*[b] and Nobuo Ikota*[a]

[a] *Redox Regulation Research Group, Research Center for Radiation Safety, National Institute of Radiological Sciences, Inage-ku, Chiba, 263-8555, Japan. E-mail: nakanis@nirs.go.jp; Fax: +81-43-255-6819; Tel: +81-43-206-3131*

[b] *Department of Material and Life Science, Graduate School of Engineering, Osaka University, SORST, Japan Science and Technology Agency (JST), Suita, Osaka, 565-0871, Japan*

[c] *Department of Physical Pharmaceutical Chemistry, Kyoritsu University of Pharmacy, Minato-ku, Tokyo, 105-8512, Japan*

[d] *Division of Organic and Bioorganic Chemistry, Kyoritsu University of Pharmacy, Minato-ku, Tokyo, 105-8512, Japan*

[e] *Division of Organic Chemistry, National Institute of Health Sciences, Setagaya-ku, Tokyo, 158-8501, Japan*

[f] *Department of Chemistry, Graduate School of Science, Osaka City University, Sumiyoshi-ku, Osaka, 558-8585, Japan*

Received 11th November 2004, Accepted 29th November 2004
First published as an Advance Article on the web 11th January 2005

The scavenging reaction of 2,2-diphenyl-1-picrylhydrazyl radical (DPPH$^{\bullet}$) or galvinoxyl radical (GO$^{\bullet}$) by a vitamin E model, 2,2,5,7,8-pentamethylchroman-6-ol (**1H**), was significantly accelerated by the presence of $Mg(ClO_4)_2$ in de-aerated methanol (MeOH). Such an acceleration indicates that the radical-scavenging reaction of **1H** in MeOH proceeds *via* an electron transfer from **1H** to the radical, followed by a proton transfer, rather than the one-step hydrogen atom transfer which has been observed in acetonitrile (MeCN). A significant negative shift of the one-electron oxidation potential of **1H** in MeOH (0.63 V *vs.* SCE), due to strong solvation as compared to that in MeCN (0.97 V *vs.* SCE), may result in change of the radical-scavenging mechanisms between protic and aprotic media.

Introduction

Recently, much attention has been paid to the mechanisms of radical-scavenging reactions of phenolic antioxidants, such as vitamin E (α-tocopherol) and flavonoids, with regard to the development of chemopreventive agents against oxidative stress and associated diseases. There are two mechanisms for the radical-scavenging reactions of phenolic antioxidants: a one-step hydrogen atom transfer from the phenolic OH group; and an electron transfer followed by a proton transfer.[1-3] Metal ions are a powerful tool that can be used to distinguish between these two mechanisms, since electron-transfer reactions are known to be significantly accelerated by their presence.[4] In fact, we have recently reported that scavenging reactions of the galvinoxyl radical (GO$^{\bullet}$) and the cumylperoxyl radical by (+)-catechin in aprotic media, such as acetonitrile (MeCN) and propionitrile, proceed *via* an electron transfer from (+)-catechin to the radicals (which is significantly accelerated by the presence of metal ions, such as Mg^{2+} and Sc^{3+}) followed by a proton transfer.[5,6] On the other hand, no effect of Mg^{2+} on the hydrogen-transfer rate from a vitamin E model, 2,2,5,7,8-pentamethylchroman-6-ol (**1H**), to 2,2-bis(4-*tert*-octylphenyl)-1-picrylhydrazyl radical (DOPPH$^{\bullet}$) or GO$^{\bullet}$ in de-aerated MeCN has been observed, indicating that the radical-scavenging reactions of **1H** in MeCN proceed *via* a one-step hydrogen atom transfer rather than *via* electron transfer.[7,8] However, the effects of solvents on the mechanism of radical-scavenging reactions of phenolic antioxidants have yet to be clarified. Leopoldini *et al.* have reported that the bond dissociation enthalpies for O–H bonds and the adiabatic ionization potentials for phenolic antioxidants, calculated with use of density functional theory, do not follow the same trends in gas, water and benzene.[2] Thus, it is of considerable importance to investigate the effects of metal ions on radical-scavenging reactions in various solvents with different polarity.[9]

We report herein that the scavenging reactions of 2,2-diphenyl-1-picrylhydrazyl radical (DPPH$^{\bullet}$) or GO$^{\bullet}$ by the vitamin E model **1H** in de-aerated methanol (MeOH) proceed *via* an electron transfer mechanism rather than *via* a one-step hydrogen atom transfer, which has been observed in de-aerated MeCN. Effects of bases on the radical-scavenging rates were also examined, to clarify whether the actual electron donor is **1H** or the corresponding phenolate anion $\mathbf{1}^-$ in MeOH. Different mechanisms in protic and aprotic solvents are discussed based on kinetic, electrochemical, and EPR data obtained in this study, providing valuable and fundamental information about the radical-scavenging mechanism of phenolic antioxidants.

Experimental

Materials

2,2,5,7,8-Pentamethylchroman-6-ol (**1H**) was purchased from Wako Pure Chemical Ind. Ltd., Japan. 2,2-Diphenyl-1-picrylhydrazyl radical (DPPH$^{\bullet}$) and galvinoxyl radical (GO$^{\bullet}$) were commercially obtained from Aldrich. Tetra-*n*-butylammonium perchlorate (Bu_4NClO_4), used as a supporting electrolyte for the electrochemical measurements, was purchased from Tokyo Chemical Industry Co., Ltd., Japan, recrystallized from ethanol, and dried under vacuum at 313 K. $Mg(ClO_4)_2$ and methanol (MeOH: spectral grade) were purchased from Nacalai Tesque, Inc., Japan and used as received. Pyridine and 2,6-lutidine were commercially obtained from Wako Pure Chemical Ind. Ltd., Japan and purified by the standard procedure.[10]

DOI: 10.1039/b416572a

Spectral and kinetic measurements

Since the phenoxyl radical of **1H** (1•) generated in the reaction of **1H** with radicals readily reacts with molecular oxygen (O_2), reactions were carried out under strictly de-aerated conditions. A continuous flow of Ar gas was bubbled through a MeOH solution (3.0 mL) containing DPPH• (4.8×10^{-5} M) and $Mg(ClO_4)_2$ (0–0.3 M) in a square quartz cuvette (10 mm id) with a glass tube neck for 10 min. Air was prevented from leaking into neck of the cuvette with a rubber septum. Typically, an aliquot of **1H** (2.0×10^{-2} M), which was also in de-aerated MeOH, was added to the cuvette with a microsyringe. This led to a reaction of **1H** with DPPH•. UV-vis spectral changes associated with the reaction were monitored using an Agilent 8453 photodiode array spectrophotometer. The rates of the DPPH•-scavenging reactions of **1H** were determined by monitoring the absorbance change at 516 nm due to DPPH• ($\varepsilon = 1.13 \times 10^4$ M^{-1} cm^{-1}) using a stopped-flow technique on a UNISOKU RSP-1000-02NM spectrophotometer. The pseudo-first-order rate constants (k_{obs}) were determined by a least-squares curve fit using an Apple Macintosh personal computer. The first-order plots of $\ln(A - A_\infty)$ *vs.* time (A and A_∞ are denoted as the absorbance at the reaction time and the final absorbance, respectively) were linear until three or more half-lives with the correlation coefficient $\rho > 0.999$. The reaction of **1H** with GO• was carried out in the same manner and the rates were determined from the absorbance change at 428 nm due to GO• ($\varepsilon = 1.32 \cdot 10^5$ M^{-1} cm^{-1}). The rate constants of the reactions in the presence of base (pyridine or 2,6-lutidine) were determined in the same manner.

Electrochemical measurements

The cyclic voltammetry (CV) and second-harmonic alternating current voltammetry (SHACV)[11-16] measurements were performed on an ALS-630A electrochemical analyzer in de-aerated MeOH containing 0.10 M Bu_4NClO_4 as a supporting electrolyte. The Pt working electrode (BAS) was polished with BAS polishing alumina suspension and rinsed with acetone before use. The counter electrode was a platinum wire. The measured potentials were recorded with respect to an $Ag/AgNO_3$ (0.01 M) reference electrode. The $E_{1/2}$ values (*vs.* $Ag/AgNO_3$) were converted to those *vs.* SCE by adding 0.29 V.[17] All electrochemical measurements were carried out at 298 K under 1 atm Ar.

EPR measurements

Typically, an aliquot of a stock solution of **1H** (2.0×10^{-2} M) in de-aerated MeOH was added to the EPR sample tube (0.8 mm id) containing a de-aerated MeOH solution of DPPH• (2.0×10^{-4} M) with a microsyringe under 1 atm Ar. EPR spectra of the phenoxyl radical 1• produced in the reaction between **1H** and DPPH• were taken on a JEOL X-band spectrometer (JES-RE1XE). The EPR spectra were recorded under non-saturating microwave power conditions. The magnitude of modulation was chosen to optimize the resolution and the signal-to-noise ratio of the observed spectra. The g values and the hyperfine splitting constants were calibrated with a Mn^{2+} marker. Computer simulation of the EPR spectra was carried out using Calleo ESR Version 1.2 program (Calleo Scientific Publisher) on an Apple Macintosh personal computer.

Results and discussion

Radical-scavenging reactions of the vitamin E model in de-aerated MeOH

Upon addition of **1H** to a de-aerated MeOH solution of DPPH•, the absorption band at 516 nm due to DPPH• disappeared immediately, accompanied by an appearance of the absorption band at 427 nm. Since the absorption band at 427 nm is diagnostic of the phenoxyl radical derived from **1H** (1•) in MeOH,[18] this spectral change indicates that hydrogen transfer from the phenolic OH group of **1H** to DPPH• takes place to produce 1• (eqn. (1)). The absorption band of 1• was shifted from 423 nm in MeCN to 427 nm in MeOH.[7,8] Such a shift in the absorption band of 1• may be due to a stronger solvation of 1• in MeOH than in MeCN.

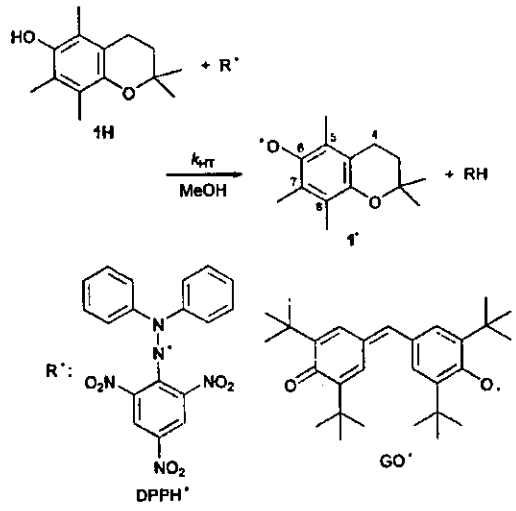

(1)

The rate of the DPPH•-scavenging reaction of **1H** was measured by monitoring the decrease in absorbance at 516 nm due to DPPH• using a stopped-flow technique. The decay of the absorbance at 516 nm due to DPPH• obeyed pseudo-first-order kinetics when the concentration of **1H** ([**1H**]) was maintained at more than a 10-fold excess of the DPPH• concentration. The pseudo-first-order rate constants (k_{obs}) increase with increasing [**1H**], exhibiting first-order dependence on [**1H**]. From the slope of the linear plot of k_{obs} *vs.* [**1H**], the second-order rate constant (k_{HT}) was determined for the radical-scavenging reaction as 1.07×10^3 M^{-1} s^{-1}, in de-aerated MeOH at 298 K. The k_{HT} value thus obtained in de-aerated MeOH is significantly larger than that determined in de-aerated MeCN (4.35×10^2 M^{-1} s^{-1}).[7] A similar result has been reported by Litwinienko and Ingold.[19] Intermolecularly hydrogen-bonded phenolic OH groups of hydrogen-bond accepting solvents, such as alcohols, are known to be essentially unreactive against radicals.[19] Thus, the enhanced k_{HT} value in MeOH suggested that the reaction mechanism in MeOH may be different from that in MeCN. The GO•-scavenging rate constant by **1H** in de-aerated MeOH has also been determined in a same manner by monitoring the decrease in absorbance at 428 nm due to GO• as 2.54×10^3 M^{-1} s^{-1}, which is slightly smaller than that in de-aerated MeCN ($3.32 \cdot 10^3$ M^{-1} s^{-1}).

Effect of magnesium ion on the rates of radical scavenging reactions

If the radical-scavenging reactions of **1H** involve an electron-transfer process as the rate-determining step, the rates of radical scavenging would be accelerated by the presence of metal ions.[5,6] This was investigated by examining the effect of $Mg(ClO_4)_2$ on the radical-scavenging rates by **1H** in de-aerated MeOH. When $Mg(ClO_4)_2$ is added to the **1H**–DPPH• system in de-aerated MeOH, the rate of DPPH•-scavenging reaction by **1H** was significantly accelerated. Such an acceleration was not observed for the DPPH•-scavenging reaction by **1H** in MeCN.[7] The k_{HT} value increases linearly with increasing Mg^{2+} concentration ($[Mg^{2+}]$) as shown in Fig. 1a. A similar acceleration effect of Mg^{2+} has been observed for the GO•-scavenging reaction by **1H** in de-aerated MeOH (Fig. 1b). Thus, the radical-scavenging reactions in de-aerated MeOH may proceed *via* an electron transfer from **1H** to DPPH• or GO•, which is accelerated by the presence of Mg^{2+}, followed by proton transfer from $\mathbf{1H}^{\bullet+}$ to $DPPH^-$ or GO^- as shown in Scheme 1. In such a case,

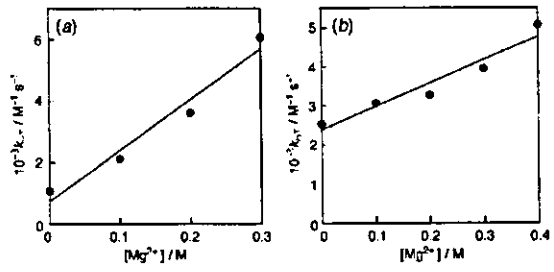

Fig. 1 Plots of k_{HT} *vs.* $[Mg^{2+}]$ in the reaction of **1H** with (a) DPPH$^{\cdot}$ and (b) GO$^{\cdot}$ in de-aerated MeOH at 298 K.

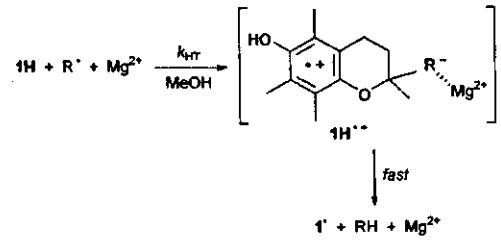

Scheme 1 Radical-scavenging reaction by **1H** *via* an electron transfer in MeOH.

the coordination of Mg^{2+} to DPPH$^{\cdot}$ or GO$^{\cdot}$ may stabilize the product, resulting in the acceleration of the electron transfer.

Effect of base on the rates of radical scavenging reactions

In protic media, such as alcohols and water, **1H** may be in equilibrium with the corresponding phenolate anion **1**$^{-}$, which is a much stronger electron donor as compared to the parent **1H**.[20] In such a case, **1**$^{-}$ may act as an electron donor rather than the parent **1H** in MeOH.

In order to clarify an actual electron donor in MeOH, the effect of base on the radical-scavenging rates of **1H** was examined. The addition of pyridine to the **1H**–DPPH$^{\cdot}$ system results in a significant increase in the rate of the DPPH$^{\cdot}$-scavenging reaction by **1H**. The k_{HT} value increases with increasing pyridine concentration to reach a constant value as shown in Fig. 2. When pyridine is replaced by 2,6-lutidine, a stronger base than pyridine, the limiting k_{HT} value is larger than that in the case of pyridine, as shown in Fig. 2. If the rate of acceleration is due to the deprotonation of the phenolic OH group of **1H** in the presence of base, the limiting k_{HT} value should be the same regardless of the basicity of pyridines. The different limiting k_{HT} values between pyridine and 2,6-lutidine in Fig. 2 suggest that little deprotonation occurs to produce **1**$^{\cdot}$ and that the actual electron donor is the parent **1H** rather than **1**$^{-}$ in MeOH, as shown in Scheme 1. In such a case, the coordination of pyridines

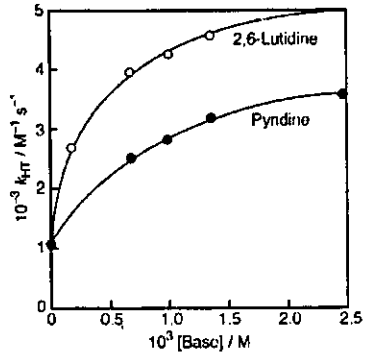

Fig. 2 Plot of k_{HT} *vs.* [base] for the reaction of **1H** with DPPH$^{\cdot}$ in the presence of pyridine (black circles) or 2,6-lutidine (white circles) in de-aerated MeOH at 298 K.

to **1H**$^{\cdot+}$ may stabilize the product, resulting in the acceleration of the initial electron-transfer process. In the presence of a large amount of a strong Lewis acid, such as $Mg(ClO_4)_2$, no deprotonation of **1H** occurs in MeOH.

Solvent effect on the one-electron oxidation potential of the vitamin E model

The solvent effect on the one-electron oxidation potential (E^0_{ox}) of **1H** was examined by cyclic voltammetry (CV) and second-harmonic alternating current voltammetry (SHACV) measurements.[11–16] Very recently, Williams and Webster have reported that the one-electron oxidation of α-tocopherol itself occurs at about 0.97 V *vs.* SCE in MeCN (0.25 M Bu_4NPF_6) based on the detailed electrochemical analyses.[21] A similar cyclic voltammogram was observed for the electrochemical oxidation of **1H** in MeCN (0.1 M Bu_4NClO_4) (data not shown), from which was determined the E^0_{ox} value (*vs.* SCE) of **1H** in MeCN as 0.97 V. On the other hand, the CV wave of **1H** in MeOH (0.1 M Bu_4NClO_4) was irreversible. Thus, SHACV measurement was carried out to determine the E^0_{ox} value of **1H** in MeOH. The E^0_{ox} value (*vs.* SCE) of **1H** in MeOH (0.1 M Bu_4NClO_4), determined from the intersection of an SHACV wave (Fig. 3), is located at 0.63 V, which is significantly more negative than the value in MeCN (0.97 V). Such a negative shift of the E^0_{ox} value in MeOH as compared to that in MeCN may be ascribed to a stronger solvation of **1H**$^{\cdot+}$ in MeOH than in MeCN. Thus, the case of one-electron oxidation of **1H** in MeOH as compared to in MeCN may result in the difference in the radical-scavenging mechanism.

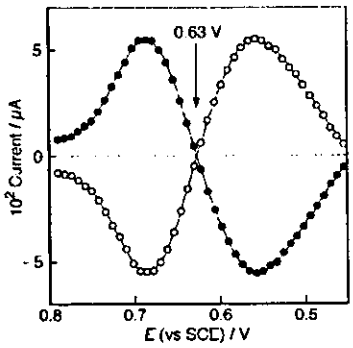

Fig. 3 SHACV of **1H** recorded at the scan rate of 4 mV s^{-1} on Pt working electrode in de-aerated MeOH (0.1 M Bu_4NClO_4) at 298 K.

EPR spectrum of the phenoxyl radical derived from the vitamin E model in de-aerated MeOH

The EPR detection of radical species derived from **1H** would provide valuable information about the solvation of the radical species.[22,23] The EPR spectrum of **1**$^{\cdot}$ in de-aerated MeOH at 298 K is shown in Fig. 4a. It should be noted that the *g* value of the EPR spectrum of **1**$^{\cdot}$ in MeOH (2.0040) is apparently smaller than that in MeCN (2.0047).[7] The observed hyperfine structure in Fig. 4a is well reproduced by the computer simulation (Fig. 4b) with four hyperfine splitting constants (*hfc*) listed in Table 1. Table 1 also shows the *hfc* values of **1**$^{\cdot}$ in MeCN.[7] All the *hfc* values in MeOH are also smaller than those in MeCN. The smaller *g* value of the EPR spectrum of **1**$^{\cdot}$ as well as the smaller *hfc* values in MeOH than those in MeCN indicates that the stronger solvation of **1**$^{\cdot}$ may occur in MeOH than in MeCN. Although the EPR spectrum of **1H**$^{\cdot+}$ could not be observed because of the fast deprotonation to produce **1**$^{\cdot}$ (Scheme 1), stronger solvation of **1H**$^{\cdot+}$ may also occur in MeOH than in MeCN, resulting in the ease of one-electron oxidation of **1H** in MeOH than in MeCN.

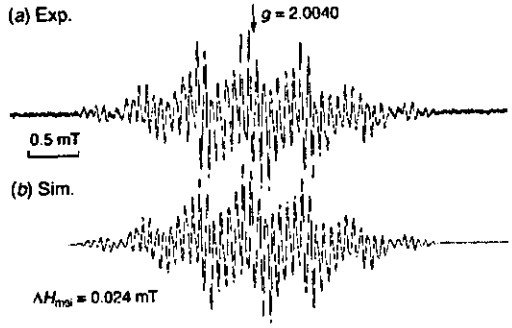

Fig. 4 (a) EPR spectrum of **1**• generated in the reaction of **1H** (1.0×10^{-3} M) with DPPH• (2.0×10^{-4} M) in de-aerated MeOH at 298 K. (b) The computer simulation spectrum. The *hfc* values used for the simulation are listed in Table 1.

Table 1 Hyperfine splitting constants (*hfc*; in mT) and *g* values of **1**• in de-aerated solvents

Solvent	*g*	$a(3H^3)$	$a(3H^7)$	$a(3H^8)$	$a(2H^4)$
MeOH	2.0040	0.577	0.423	0.073	0.126
MeCN	2.0047[a]	0.587[a]	0.440[a]	0.086[a]	0.139[a]

[a] Taken from ref. 7.

In conclusion, the scavenging reaction of DPPH• or GO• by **1H** in MeOH proceeds *via* the electron transfer from **1H** to DPPH• or GO• followed by proton transfer rather than *via* the one-step hydrogen atom transfer, which has been observed in MeCN. Such a difference in the mechanism of radical-scavenging reactions by the vitamin E model depending on the solvents provides valuable information for the biological antioxidative reactions.

Acknowledgements

This work was partially supported by a Grant-in-Aid for Scientific Research (A) (No. 16205020) and a Grant-in-Aid for Young Scientist (B) (No. 15790032) from the Ministry of Education, Culture, Sports, Science and Technology, Japan.

References

1 J. S. Wright, E. R. Johnson and G. A. Di Labio, *J. Am. Chem. Soc.*, 2001, **123**, 1173.
2 M. Leopoldini, T. Marino, N. Russo and M. Toscano, *J. Phys. Chem. A*, 2004, **108**, 4916.
3 M. Leopoldini, I. P. Pitarch, N. Russo and M. Toscano, *J. Phys. Chem. A*, 2004, **108**, 92.
4 S. Fukuzumi, in *Electron Transfer in Chemistry*, ed. V. Balzani, Wiley-VCH, New York, 2001, vol. 4, pp. 3–67.
5 I. Nakanishi, K. Miyazaki, T. Shimada, K. Ohkubo, S. Urano, N. Ikota, T. Ozawa, S. Fukuzumi and K. Fukuhara, *J. Phys. Chem. A*, 2002, **106**, 11123.
6 I. Nakanishi, K. Ohkubo, K. Miyazaki, W. Hakamata, S. Urano, T. Ozawa, H. Okuda, S. Fukuzumi, N. Ikota and K. Fukuhara, *Chem. Res. Toxicol.*, 2004, **17**, 26.
7 I. Nakanishi, K. Fukuhara, T. Shimada, K. Ohkubo, Y. Iizuka, K. Inami, M. Mochizuki, S. Urano, S. Itoh, N. Miyata and S. Fukuzumi, *J. Chem. Soc., Perkin Trans. 2*, 2002, 1520.
8 I. Nakanishi, S. Matsumoto, K. Ohkubo, K. Fukuhara, H. Okuda, K. Inami, M. Mochizuki, T. Ozawa, S. Itoh, S. Fukuzumi and N. Ikota, *Bull. Chem. Soc. Jpn.*, 2004, **77**, 1741.
9 H.-Y. Zhang and L.-F. Wang, *J. Phys. Chem. A*, 2003, **107**, 11258.
10 D. D. Perrin, W. L. F. Armarego and D. R. Perrin, *Purification of Laboratory Chemicals, 4th Edition*, Pergamon Press, Elmsford, New York, 1996.
11 T. G. McCord and D. E. Smith, *Anal. Chem.*, 1969, **41**, 1423.
12 A. M. Bond and D. E. Smith, *Anal. Chem.*, 1974, **46**, 1946.
13 M. R. Wasielewski and R. Breslow, *J. Am. Chem. Soc.*, 1976, **98**, 4222.
14 E. M. Arnett, K. Amarnath, N. G. Harvey and J.-P. Cheng, *J. Am. Chem. Soc.*, 1990, **112**, 344.
15 M. Patz, H. Mayr, J. Maruta and S. Fukuzumi, *Angew. Chem., Int. Ed. Engl.*, 1995, **34**, 1225.
16 S. Fukuzumi, N. Satoh, T. Okamoto, K. Yasui, T. Suenobu, Y. Seko, M. Fujitsuka and O. Ito, *J. Am. Chem. Soc.*, 2001, **123**, 7756.
17 K. Mann and K. K. Barnes, in *Electrochemical Reactions in Nonaqueous Systems*, Marcel Dekker Inc., New York, 1990.
18 K. Mukai, Y. Watanabe and K. Ishizu, *Bull. Chem. Soc. Jpn.*, 1986, **59**, 2899.
19 G. Litwinienko and K. U. Ingold, *J. Org. Chem.*, 2003, **68**, 3433.
20 I. Nakanishi, K. Miyazaki, T. Shimada, Y. Iizuka, K. Inami, M. Mochizuki, S. Urano, H. Okuda, T. Ozawa, S. Fukuzumi, N. Ikota and K. Fukuhara, *Org. Biomol. Chem.*, 2003, **1**, 4085.
21 L. L. Williams and R. D. Webster, *J. Am. Chem. Soc.*, 2004, **126**, 12441.
22 T. Yonezawa, T. Kawamura, M. Ushio and Y. Nakao, *Bull. Chem. Soc. Jpn.*, 1970, **43**, 1022.
23 M. Lucarini, V. Mugnaini, G. F. Pedulli and M. Guerra, *J. Am. Chem. Soc.*, 2003, **125**, 8318.